The autotaxin-LPA₂ GPCR axis is modulated by γ-irradiation and facilitates DNA damage repair

Andrea Balogh[1], **Yoshibumi Shimizu**[1], **Sue Chin Lee**[1], **Derek D. Norman**[1], **Ruchika Gangwar**[1], **Mitul Bavaria**[1], **ChangSuk Moon**[1,#], **Pradeep Shukla**[1], **Radakrishna Rao**[1], **Ramesh Ray**[1], **Anjaparavanda P. Naren**[1,#], **Souvik Banerje**[2], **Duane D. Miller**[2], **Louisa Balazs**[3], **Louis Pelus**[4], and **Gabor Tigyi**[1,&]

[1]Department of Physiology, University of Tennessee Health Sciences Center Memphis, 894 Union Avenue, Memphis, TN, 38163 USA

[2]Department of Pharmaceutical Sciences, University of Tennessee Health Sciences Center Memphis, 894 Union Avenue, Memphis, TN, 38163 USA

[3]Department of Pathology and Laboratory Medicine, University of Tennessee Health Sciences Center Memphis, 894 Union Avenue, Memphis, TN, 38163 USA

[4]Department of Microbiology & Immunology, Indiana University School of Medicine, 950 West Walnut Street, R2-302, Indianapolis, IN, 46202, USA

Abstract

In this study we characterized the effects of radiation injury on the expression and function of the autotaxin (ATX)-LPA₂ GPCR axis. In IEC-6 crypt cells and jejunum enteroids quantitative RT-PCR showed a time- and dose-dependent upregulation of lpa2 in response to γ-irradiation that was abolished by mutation of the NF-κB site in the lpa2 promoter or by inhibition of ATM/ATR kinases with CGK-733, suggesting that lpa2 is a DNA damage response gene upregulated by ATM via NF-κB. The resolution kinetics of the DNA damage marker γ-H2AX in LPA-treated IEC-6 cells exposed to γ-irradiation was accelerated compared to vehicle, whereas pharmacological inhibition of LPA₂ delayed the resolution of γ-H2AX. In LPA₂-reconstituted MEF cells lacking LPA₁&₃ the levels of γ-H2AX decreased rapidly, whereas in Vector MEF were high and remained sustained. Inhibition of ERK1&2 or PI3K/AKT signaling axis by pertussis toxin or the C₃₁₁A/C₃₁₄A/L₃₅₁A mutation in the C-terminus of LPA₂ abrogated the effect of LPA on DNA repair. LPA₂ transcripts in Lin⁻Sca-1⁺c-Kit⁺ enriched for bone marrow stem cells were 27- and 5-fold higher than in common myeloid or lymphoid progenitors, respectively. Furthermore, after irradiation higher residual γ-H2AX levels were detected in the bone marrow or

jejunum of irradiated LPA$_2$-KO mice compared to WT mice. We found that γ-irradiation increases plasma ATX activity and LPA level that is in part due to the previously established radiation-induced upregulation of TNFα. These findings identify ATX and LPA$_2$ as radiation-regulated genes that appear to play a physiological role in DNA repair.

Graphical abstract
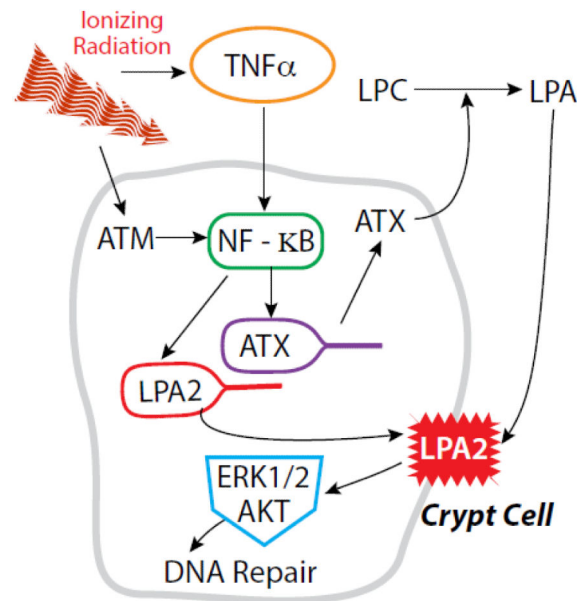
Keywords

DNA damage repair; lysophosphatidic acid; ATX; LPA$_2$; γH2AX; NF-κB

Introduction

Radiation induced DNA double-strand breaks (DSB) are detected by ataxia telangiectasia mutated kinase (ATM), which induces the activation of cell-cycle check points to allow DNA damage repair, cell survival, and stress response pathways [1, 2]. The decision between survival and apoptosis of a cell exposed to a genotoxic insult depends on the stress signals and also on inputs from the cell microenvironment [3]. Radiation protectors are compounds that prevent radiation injury when applied before exposure whereas, radiation mitigators are compounds that can be administered after radiation exposure to attenuate injury. Mechanistically, radiation mitigator compounds are aimed at enhancing those innate signaling pathways which lead to DNA damage repair (DDR), inhibition of apoptosis, and enhancement of cell survival.

The lysophosphatidic acid G protein coupled receptor subtype 2 (LPA$_2$ GPCR) is a member of endothelial differentiation gene (EDG) family showing more than 80 % homology to LPA$_1$ and LPA$_3$ [4, 5]. The natural ligand of LPA$_2$ is lysophosphatidic acid (LPA) a growth factor like molecule abundantly present in biological fluids. LPA is produced primarily from

lysophosphatidylcholine (LPC) by the lysophospholipase D enzyme designated autotaxin (ATX) [6-8]. LPA_2 is the most sensitive GPCR to LPA stimulation with an EC_{50} of ~1.4 nM. LPA_2 is expressed in a wide range of cell types including hematopoietic [9, 10] and embryonic stem cells [11]. LPA_2 was shown to prevent and also to mitigate apoptosis elicited by serum withdrawal, or genotoxic stressors including chemotherapeutics, and radiation-induced DNA damage [12-14]. LPA_2 is overexpressed in different tumors thereby conferring resistance to radiation- and chemotherapy [15-17].

Our group has synthesiozed LPA_2-specific agonist compounds with the ultimate goal of developing drugs that can prevent and/or mitigate radiation-injury resulting from exposure to high levels of radiation that elicit the hematopoietic (HE) and the gastrointestinal (GI) acute radiation syndromes (ARS) [13, 18-22]. Stimulation of LPA_2 among others leads to activation of MAPK/ERK, PI3K/AKT and NF-κB signaling pathways resulting in enhanced cell survival, proliferation, and migration that are important events in radiation injury repair [4, 14, 23-25].

The objective of the present study was to characterize the effects of radiation injury on expression and function of the ATX-LPA_2 axis in cultured cells and in mice exposed to total body γ-irradiation (TBI) from a ^{137}Cs source. Specifically, we examined the transcriptional regulation of *lpa2* in IEC-6 crypt-derived cells and in crypts isolated from the small intestine of mice in response to ionizing radiation and evaluated the impact of such regulation on the DNA damage response (DDR). Radiation-induced upregulation of *lpa2* was mediated by ATM-dependent activation of NF-κB transcription. We found that LPA_2 was dose- and time-dependently upregulated in response to γ-radiation. LPA_2 expression and activation augmented the repair of DSB monitored by the resolution of phosphorylated histone 2AX (γH2AX) in vitro and in vivo. In addition, we evaluated the effect of radiation on LPA production via ATX in blood, white adipose tissue (WAT), and the liver of wild type (WT) mice. We found that mice exposed to 6 Gy TBI γ-irradiation ATX activity increased within 4 h, resulting in an increase in plasma LPA levels that favors a radiation-induced acute regenerative tissue response. We also found that generation of TNFα accompanying radiation exposure upregulated ATX expression in IEC-6 cells. γH2AX resolution was delayed in LPA_2 knockout (KO) mice compared to WT C57BL/6 mice. These results indicate that ATX and LPA_2 are regulated by γ-irradiation and play a role in the endogenous DNA damage response and repair pathways.

Methods

Materials

LPA 18:1, 1-Heptadecanoyl-LPC (17:0), and 1-heptadecanoyl-LPA (17:0) was purchased from Avanti Polar Lipids (Alabaster, AL, USA). A stock solution of LPA (2 mM) was prepared with equimolar complex with charcoal-stripped, fatty acid-free bovine serum albumin (BSA, Sigma-Aldrich; St. Louis, MO, USA) in phosphate-buffered saline (PBS). The LPA_2-specific antagonist Amgen compound 35 reported by Beck et al. and the LPA_2-specific agonist compound 11d (designated radioprotectin 1, RP-1) were synthesized as described previously [21, 26]. The FS-3 ATX substrate was from Echelon Biosciences (Salt Lake City, UT, USA). LY294002 was purchased from Cell Signaling Technology (Danvers,

MA, USA), U0126 from Promega (Madison, WI, USA), pertussis toxin from LIST Biological Laboratories, Inc. (Campbell, CA, USA), CGK-733 from Calbiochem (San Diego, CA, USA).

Culture and irradiation of IEC-6 cells

IEC-6 non-transformed crypt-derived rat embryonic intestinal epithelial cells at passage 17 were plated in 6-well plates at a density of 10^5 cells/well in 1.5 ml complete culture medium as described previously [18]. The next day, cells were irradiated with 5, 10, or 15 Gy γ-irradiation from a ^{137}Cs source at a dose rate of 4.4 Gy/min. After irradiation, the culture medium was replaced with fresh complete culture medium. Cells were harvested for RNA isolation using the RNeasy Mini Kit (Qiagen, Valencia, CA, USA) at 12, 24, or 36 h after irradiation.

Generation of mouse embryonic fibroblast (MEF) cells from LPA$_1$ × LPA$_2$ double KO mice reconstituted with the human LPA$_2$ ortholog

Very few cell lines lack LPA GPCR. To generate a radiation-sensitive cell platform that lacks the EDG family LPA GPCR we generated a MEF cell line from LPA$_1$ × LPA$_2$ double KO mice that also lack endogenous LPA$_3$ expression and transduced them with lentiviral constructs of the human LPA$_2$ ortholog (LPA$_2$ MEF) or an empty vector (Vector MEF) [24] . We used LPA$_2$ and Vector MEF cells to evaluate the effects of LPA$_2$ activation on DDR as we described [19, 22].

Isolation and culture of intestinal crypts

The animal protocols used in the present study were reviewed and approved by the Institutional Animal Use and Care Committee of the University of Tennessee Health Science Center Memphis. The small intestine was removed from euthanized 8 week-old C57BL/6 mice and washed with cold PBS. After opening the small intestine, villi were scraped off and discarded before the tissue was cut into small pieces. After several rinses with cold PBS, the tissue was incubated at 4°C with 2 mM EDTA in PBS for 30 min and passed through a cell strainer with 70 μm pore size (BD Biosciences, San Jose, CA, USA). Subsequently, the crypts that passed through the strainer were collected by centrifugation at 400 × g for 5 min and washed with enteroid medium (Gibco, Grand Island, NY, USA) including 1x Glutamax, 20 units/ml penicillin, 20 μg/ml streptomycin, 10mM HEPES, (all supplements from Gibco) without growth factors and centrifuged at 400 × g for 2 min. After discarding the supernatant, the isolated crypts were resuspended with Matrigel (BD Biosciences) and plated in 24-well -plates. Enteroid medium (500 μl) supplemented with 1xB27 (Gibco) 1xN2 (Gibco), 1mM N-acetyl cysteine (Sigma-Aldrich), 100ng/ml Noggin, (PeproTech, Rocky Hill, NJ, USA), 1μg/ml R-spondin-1, (R&D Systems, Minneapolis, MN, USA) and 50ng/ml EGF (R&D Systems) were added to the crypts in the hardened Matrigel. The enteroids were incubated at 37°C in the presence of 5% CO_2-95% air atmosphere for 24 h and irradiated with 4 Gy at a dose rate of ~ 0.85 Gy/min.

Quantitative RT-PCR (QPCR)

Total RNA (1.5 μg) was used for the synthesis of cDNA using the ThermoScript RT-PCR system for first strand synthesis (Invitrogen – Life Technologies, Grand Island, NY, USA). QPCR reactions were performed using cDNA mix (cDNA corresponding to 35 ng RNA) with 300 nmol of the primers in a final volume of 25 μl of $2 \times$ concentrated RT2 Real-Time SYBR Green/ROX master mix (Qiagen) in an Applied Biosystems 7300 Real-Time PCR instrument (Norwalk, CT, USA). The cycle parameters were: 50°C for 2 minutes, one denaturation step at 95°C for 10 minutes and 40 cycles of denaturation at 95°C for 10s followed by annealing and elongation at 60°C. Relative gene expression of each transcript was normalized to GAPDH using the Ct method. Primer sequences for GAPDH were: forward: 5′-CTGCACCACCAACTGCTTAG-3′, reverse: 5-GGGCCATCCACAGTCTTCT-3, and for LPA$_2$: forward 5-CCAGCCTGCTTGTCTTCCTA-3, and reverse: 5-GTGTCCAGCACACCACAAAT-3. For ATX gene product QPCR measurements 0.1×10^6 IEC-6 cells were plated per well of a 6-well plate in complete growth media. The following day, cells were serum-starved for 24 hours prior to stimulation with 10ng/ml of rat TNFα (R&D Systems) for 15 min, 3 h and 6h. The ATX forward primer was 5′-ATTACAGCCACCAAGCAAGG-3′ and the reverse 5′-GGCAGAGAAAGCCACTGAAG -3′.

Construction and assay of a luciferase reporter plasmid containing the human LPA$_2$ promoter

The human LPA$_2$ promoter sequence between base pairs −965/+139 was amplified from 50 ng of human genomic DNA with Kod hot start polymerase (Novagen, Madison, WI, USA) with the primers: LPA$_2$-forward: 5-GTAGAGACGGGGTTTCAGCATG-3 and LPA$_2$-reverse: TATAAGCTTCTGGGCCTCCAGTCACGCC, with an added HindIII restriction site to the reverse primer. The PCR product was cloned into pGL 4.10(luc2) (Promega) between the EcoRV and HindIII restriction sites. Site-directed mutagenesis of the NF-κB sites was done with the Quick Change kit (Stratagene, La Jolla, CA, USA). The consensus binding site: GGGGCTCCCC was changed into GTGATTCTCC with the forward primer 5-GCCGTGGAGGCGTGATTCTCCCAGGTGGCGGG -3 and reverse primer 5-CCCGCCACCTGGGAGAATCACGCCTCCACGGC-3. The promoter constructs containing firefly luciferase were cotransfected into HEK293T cells in triplicate with pGL4.74[hRluc/TK] (Promega) containing renilla luciferase as internal control using Lipofectamine 2000 (Life Technologies) reagent. As a positive control for radiation-induced NFκB activation cells were transfected with pGL4.32[Luc2P/ NFκB-RE/Hygro] (Promega). Relative activities (Firefly/Renilla luciferase activity) were determined 24 hours after transfection using Dual Glow kit (Promega).

Measuring LPA$_2$-activation using ligand-induced Ca^{2+}-mobilization assay

To determine the LPA$_2$ responsiveness of irradiated IEC-6 cells to ligand-activation Ca^{2+} mobilization assays were used. We generated dose-response curves using the LPA$_2$-specific agonist compound designated Radioprotectin-1 (RP-1) reported in our previous publication by Patil et al. [21]. Fura-2AM-loaded IEC-6 cells were exposed to 0.03-10 μM RP-1 in

quadruplicate wells. Ligand-mediated rise in intracellular Ca^{2+} was measured using a Flex Station 2 robotic fluorescent plate reader (Molecular Devices) as described previously [18].

Flow cytometric determination of γ-H2AX in IEC-6 cells

IEC-6 cells were grown in complete medium supplemented with 10 μg/ml insulin as described previously [18]. Prior to 15 Gy γ-radiation cells were serum starved overnight and treated with 10 μM LPA or vehicle (0.1% BSA). After irradiation the medium was replaced with serum-free medium containing either LPA or vehicle. At the indicated time points (0.5, 1, 2, 4, 6, 8 hours post radiation) cells were trypsinized, washed with cold PBS and stained with anti-human/mouse phospho-H2AX (residue S139, γH2AX) labeled with eFluor660 (eBioscience, San Diego, CA) using the Foxp3/Transcription Factor Staining Buffer Set (Biolegend, San Diego, CA) and protocol. For inhibition of the LPA_2 receptor, the cells were treated with 0.2 μM or 1 μM of the LPA_2 antagonist compound 35 for 30 min followed by 15 min of 10 μM LPA treatment prior to irradiation. After irradiation the culture medium was changed to fresh medium, containing the antagonist and LPA. Cells were harvested and stained for γH2AX 6 h after irradiation. Fluorescence was measured using a LSR II instrument (Becton Dickinson Inc., Franklin Lakes, NJ) and analyzed with the FACSDiva software (Becton Dickinson Inc.).

Isolation of hematopoietic stem cell and progenitor cell and qPCR analysis of LPA_2 receptor expression

For purification of hematopoietic stem cell and progenitor cell populations, femurs and tibias from C57Bl/6 mice were flushed with 5 ml Iscove's modified Dulbecco's medium containing 2% fetal bovine serum and a single cell suspension was prepared by passing through a 26 g needle. Lineage-positive cells were depleted using the lineage-cell depletion kit (Miltenyi Biotec, Auburn, CA, USA) and lineage-negative cells were stained with fluorochrome-conjugated antibodies against Sca-1, c-Kit, IL-7Rα, CD34 and FCRγII/III. Hematopoietic stem cell enriched LSK (Lin−Sca-1+c-Kit+), common myeloid progenitor (CMP) enriched (Lin−Sca-1−IL-7R−c-Kit+FCR γll/lll^low CD34+) and lymphoid progenitor cell enriched (Lin−Sca-1^int c-Kit^int IL-7R+ CD34+) cell populations were sorted on a FACS Aria (BD Bioscience, San Jose, CA, USA), collected in PBS and cell pellets frozen at −80°C. All antibodies were purchased from BD Biosciences or eBiosciences.

RNA was isolated from cells with RNeasy Micro kit (Qiagen). RNA concentration and quality were assessed with Nanodrop (Thermo-Fischer Scientific, Waltham, MA, USA). 50 ng total RNA were converted to SPIA amplified cDNA using the Ovation PicoSL WTA System V2 (NuGEN Technologies, San Carlos, CA, USA) according to the manufacturer's protocol. The amplified SPIA cDNA was purified with Qiagen QIAquick PCR purification column (Qiagen) according to modifications from NuGEN. Quantitative PCR reactions were carried out in triplicate using 2 ng of SPIA amplified cDNA with 300 nmol of each primer in a final volume of 25 μl of 2 × Maxima SYBR Green/ROX qPCR master mix (Thermo Fischer Scientific). Amplification was performed after one initial step of 10 min at 95 °C for 40 cycles at 94°C /15 s and 60°C /60 s with StepOnePlus real-time PCR system (Applied Biosystems). Relative gene expression of each mRNA to HPRT was determined using the dCt method. The HPRT primer sequence used were: Forward 5′-

AAGGACCTCTCGAAGTGTTGGATA-3′, and reverse 5′-
CATTTAAAAGGAACTGTTGACAACG-3′.

Flow cytometric determination of γH2AX in mouse bone marrow

Gender- and age-matched eight-to-ten-week-old WT and LPA$_2$ KO (kind gift of Dr. Jerold Chun, Scripps Institute, La Jolla, CA) mice were exposed to 6 Gy TBI γ-radiation at a dose rate of 80 cGy/min. Bone marrow was removed from the tibia and femur of one leg by flushing the bones with PBS. After lysis of erythrocytes with ACK lysis buffer (Invitrogen – Life Technologies), bone marrow cells were fixed and permeabilized with the FoxP3 Fix/ Perm kit and stained with anti-human/mouse γH2AX antibody labeled with PerCP-eFluor710 (eBioscience). Flow cytometric measurements and analysis was done as described above.

Immunofluorescence staining for γH2AX of jejunum and IEC-6 cells

Cryo-sections of jejunum (12 μm thickness) were fixed in acetone methanol mixture (1:1) at −20°C for 2 min and rehydrated in PBS. Sections were permeabilized with 0.2% Triton X-100 in PBS for 15 min and blocked in 4% non-fat milk in TBST (20mM TRIS, pH 7.2 and 150 mM NaCl). Sections were incubated with anti-rabbit γH2AX (Cell Signaling) at room temperature for 1 h, washed 3 times in 1 % milk in TBST, then incubated with the Cy3 conjugated anti-rabbit IgG (Sigma-Aldrich) diluted 1:100 in 4 % milk in TBST for 1 hour at room temperature in the dark. Cells were washed with PBS and counterstained with Hoechst 33342 (Sigma-Aldrich). Fluorescence was visualized by confocal microscopy using a Zeiss LSM 5 microscope and images from x-y sections (1 μm) were collected using the Zen software (Zeiss, Göttingen, Germany).

For γH2AX detection in IEC-6 cells a total of 7×10^5 cells were grown in 24-well plates on 13-mm glass cover slips and serum starved overnight. The next morning, cells were treated with 1 μM LPA$_2$ antagonist for 1 hour and subsequently with 10 μM LPA or vehicle (0.1% BSA) for 15 minutes prior to irradiation with 15 Gy.

Cells were washed twice in ice cold PBS and fixed with methanol : acetone (1:1). Following permeabilization in 0.2% Triton-X in PBS for 15 min, cells were washed 3 times in PBS and blocked with 4 % milk in TBST. Cells were incubated with anti-rabbit γH2AX (1:400; Cell Signaling) at room temperature for 1 h, washed 3 times in 1 % milk in TBST, and incubated with the secondary fluorescent conjugated antibody (antirabbit Cy3 conjugated anti-rabbit IgG; Sigma) diluted 1:100 in 4 % milk in TBST for 1 hour at room temperature in dark. Cells were washed with PBS and stained with DAPI. Cells were visualized by confocal microscopy as above and analyzed with the ImageJ software (NIH).

Western blotting

Cell lysates were prepared in M-PER buffer (Thermo-Fisher Scientific) supplemented with Proteinase Phosphatase Inhibitor Cocktail (Sigma-Aldrich). Protein concentration was determined with a BCA protein assay kit (Thermo-Fisher Scientific) using BSA as standard. Equal amounts of cell lysates were fractionated on 10% SDS-PAGE gels and transferred to nitrocellulose membrane. The membranes were blocked with 5% (W/V) milk in TBST for 1

h before overnight probing with antibodies. Subsequently the membranes were washed in TBST and reacted with the appropriate horseradish peroxidase–conjugated secondary antibodies and developed using the Pierce™ SuperSignal West Pico ECL kit (Thermo-Fisher Scientific). Antibodies to total and phosphorylated forms of AKT, ERK1/2 and γH2AX, were purchased from Cell Signaling and the antibody to β-actin was from Sigma-Aldrich.

Determination of autotaxin activity

Heparin-anticoagulated plasma (5 μl) or tissue homogenate (20 μg protein, dissolved in 20 μl of 10 mM TRIS-HCl, (pH 7.4) with protease inhibitor cocktail) was incubated with 2 μM FS-3 substrate and 10 μM BSA in a total 60 μl of assay buffer consisting of 50 mM TRIS-HCl, 140 mM NaCl, 5 mM KCl, 1mM $CaCl_2$, and 1 mM $MgCl_2$ (pH 8.0) for 4 h at 37°C. The fluorescence ($\lambda_{excitation}$= 485 nm and $\lambda_{emission}$ = 538 nm) was recorded every 2 min by a FlexStation 2 plate reader. Reaction rates were calculated based on the slope of the linear portion of the reaction curves and reported as ATX activity in terms of RFU/min. ATX activity between sham and irradiated samples was compared via Student's t-test for plasma, WAT, and liver samples. Measurement of ATX activity in conditioned media:

To determine the effect of TNFα on ATX activity in IEC-6 cells, 0.9×10^6 cells were plated per 10 cm dish in complete growth medium and cultured for 2 days. Growth medium was replaced with serum-free medium for 24 h followed by stimulation with 10 ng/ml of rat TNFα for 24 hours. Conditioned medium was collected, centrifuged, filtered through a 0.22μm filter unit and concentrated (~40 fold) using the Amicon Ultra 30 KDa-cutoff Centrifugal Filter Units (Millipore). Control conditioned medium was generated from cells not exposed to TNFα stimulation. ATX activity was measured by incubating 20μL of concentrated conditioned medium in the presence of 10μM BSA and 2μM FS-3 in triplicates after a 4 h incubation period.

Lipid extraction and determination of LPC and LPA from plasma and tissues

LPC and LPA were extracted according to the method of Okudaira et al. [27]. In brief, 0.02 ml of the EDTA-treated mouse plasma was placed in 1.5-mL siliconized sample tubes. Acidic methanol (0.09 ml, pH 4) containing 0.03 nmol 17:0-LPA and 7.5 nmol 17:0-LPC was added to the plasma samples. This mixture was sonicated for 3 min in a bath sonicator. After centrifugation at $16,100 \times g$ for 10 min at 4°C, the supernatants were collected and analyzed by LC-MS/MS.

The ground tissues were vigorously shaken with 9 times the volume (μL/mg V/W) of acidic methanol (pH 4) containing 17:0-LPA (0.3 nmol) and 17:0-LPC (75 nmol) and 150 mg of 1.0 mm zirconium oxide beads for 10 min at 4°C. This homogenate was sonicated for 3×30 s in a bath sonicator. After an initial centrifugation at $1,000 \times g$ for 10 min at 4°C, the supernatants were recentrifuged at $16,100 \times g$ for 10 min at 4°C. The supernatant was filtered using a 0.2μm captiva premium syringe filter from Agilent Technologies (Santa Clara, CA, USA) and subjected to the LC-MS/MS. LC-MS/MS was performed using an ABI Sciex (Foster City, CA, USA) API4500 mass spectrometer with an HTC-xt PAL autosampler (CTC Analytics, Zwingen, Switzerland) connected to an LC-30AD HPLC pump (Shimadzu, Kyoto, Japan), CTO-30A column oven (Shimadzu), CBM-20A controller

(Shimadzu). LPC in the lipid extract were separated on an Ascentis Express C18 column (2.7 μm, 2.1 × 150 mm; Supelco, Bellefonte, PA, USA) developed with an isocratic solvent system of methanol-water mixture (19:1, v/v) containing 5 mM ammonium formate (Solvent A), sample injection volume was 5 μl at 0.2 ml/min. The molecular species of LPA in the extract were separated on an ODS-100Z column (5 μm, 2.0 × 150 mm; Tosoh, Tokyo, Japan) with Solvent A, sample injection volume was 5 μl at 0.22 ml/min. For quantification, LPC was analyzed by positive ion electrospray ionization with multiple reaction monitoring (MRM) of parent ($[M + H]^+$)/daughter ($[phosphocholine]^+$) at m/z 184, where M is the molecular weight of the parent species. LPA species were quantified in ESI- with MRM of parent ($[M - H]^-$)/daughter ions ($[cyclic\ glycerophosphate]^-$) at m/z 153. Quantification was accomplished by referencing peak areas to those of the internal standards. Conditions of MRM analysis for LPC were as follows: curtain gas 50, CAD gas 8, IS voltage 5000V, source temperature 500°C, GS1 30, GS2 80, DP 90, EP 10, CE 33, and CXP 13. Conditions of MRM analysis for LPA were as follows: curtain gas 20, CAD gas 8, IS voltage –4500V, source temperature 700°C, GS1 30, GS2 80, DP –80, EP –6, CE –30, and CXP –7.

Irradiation of mice

The total-body irradiation (TBI) protocol was reviewed and approved by the University of Tennessee Health Science Center Animal Care and Use Committee. Irradiations were performed using a ^{137}Cs source (J.L. Shepherd & Assoc. Mark I, Model 25, San Fernando, CA, USA). Animals placed in a rotating turntable mouse holder received 6 Gy total body irradiation at a dose rate of 76 cGy/min and sacrificed 15 min, 4 h, and 24 h post-irradiation. Radiation field mapping and calibration by ion chamber dosimetry was done by manufacturer at installation. In addition, routine validation and quality control measurements of exposure rates and exposure rate mapping in the chamber at positions of interest was conducted by a Certified Health Physicist using a calibrated RadCal 0.6 cc therapy grade ion chamber/electrometer system. High-dose thermoluminescent dosimeters were used in most irradiations to validate the actual dose delivered to the mice (MD Anderson Cancer Center Radiation Dosimetry Services). The isodose field was validated using Gafchromic film for high-dose dosimetry (10-50 Gy, Ashland Inc., Covington, KY).

Results

Induction of lpa2 expression by γ-irradiation

We tested the hypothesis that ionizing radiation regulates the expression of the *lpa2* transcript using QPCR. In the IEC-6 crypt-derived primary epithelial cell line QPCR analysis revealed that following γ-irradiation *lpa2* transcripts increased in a time- and dose-dependent manner (Fig.1A). Increased expression of *lpa2* was observed at all doses between 5 – 15 Gy, beginning the earliest at 12 h postirradiation with a maximal induction of ~4.5-fold at 24 h postirradiation after 15 Gy exposure (Fig. 1A). A similar upregulation trend was seen in *lpa2* expression following 4 Gy γ-irradiation of cultured enteroids that are representative of crypts enriched in stem cells. In cultured enteroids, *lpa2* showed a 2-fold increase relative to the control one day after IR treatment (Fig. 1B).

We and others have reported previously that LPA_2 protects cells from apoptosis induced by genotoxic stress as a result of radiation and chemotherapeutic drugs [12-14, 28]; however, no direct evidence has been reported about the effects of LPA_2 on DDR. To assess the potential implications of LPA_2 upregulation in radiation-induced DDR we treated IEC-6 cells with CGK-733, an ATM/ATR kinase inhibitor and quantified induction of *lpa2* transcripts by QPCR (Fig. 1C). Our results indicate that the transcriptional regulation of *lpa2* in response to radiation is dependent, at least in part, on ATM because CGK-733 dose-dependently blocked the radiation-induced upregulation. At 5 μM concentration CGK-733 completely abolished the radiation-induced upregulation of *lpa2* transcripts.

To elucidate the transcription-factor pathway responsible for the upregulation of the *lpa2* gene, we performed an *in silico* search using the Transfac software (Qiagen) for predicted transcription factor binding sites in the human *lpa2* promoter. The NF-κB consensus binding site 5′-CGGGGCTCCCCCC-3′ at position −62 from the transcription initiation site indicated that the lpa2 promoter could be regulated by the NF-κB pathway in response to γ-irradiation. Because radiation-induced DNA-damage is known to activate ATM that in turn upregulates the transcriptional activity of NF-κB [29], the link between radiation-induced *lpa2* upregulation via NF-κB offers a testable hypothesis and extends our observations shown in figure 1C for the role of ATM in this pathway. Mutation of this binding GGGGCTCCCC site to GTGATTCTCC abolished the radiation-induced upregulation of a reporter gene construct transfected into HEK293T cells (Fig. 1D). This result is consistent with the role of NF-κB in the radiation-induced upregulation of the *lpa2* transcript.

Despite the significant increase in the abundance of *lpa2* transcripts it is possible that protein may not increase or due to the high radiation dose applied, the LPA_2 receptor might not be functional. To assess the functionality of the LPA_2 GPCR pathway we used ligand-activated Ca^{2+} assay to measure the response of irradiated IEC-6 cells to the LPA_2-specific agonist compound RP-1 [21]. Irradiated IEC-6 cells gave significantly higher Ca^{2+} responses to compound RP-1 than the non-irradiated cells shifting the dose-response curve to the left, indicating that was LPA_2 remains functional and is upregulated in irradiated IEC-6 cells (Fig 2A).

Activation of LPA_2 accelerates resolution of radiation-induced γH2AX in IEC-6 cells

The modified histone γH2AX is a sensitive biomarker for the detection of DNA damage. The presence of γH2AX foci indicates DSB, whereas resolution of γH2AX correlates with the repair of DNA breaks [30, 31].

To examine whether LPA_2 is involved in radiation-induced DNA damage repair, we used flow cytometry to quantify γH2AX in IEC-6 cells exposed to radiation. As shown in figure 2B the percentage of γH2AX positive cells peaked within the first hour after radiation and it was lower compared to vehicle treated cells at all subsequent times tested. This effect was most evident in LPA treated cells compared to vehicle treatment at 6 h and 8 h post radiation showing a significantly faster resolution of γH2AX in LPA treated cells compared to vehicle treatment. As IEC-6 cells express multiple subtypes of LPA GPCR [12] to confirm the contribution of LPA_2 in γH2AX resolution, we treated IEC-6 cells with the LPA_2 specific antagonist Amgen compound 35 [26] and quantified γH2AX level at 6 h after irradiation

with 15 Gy using flow cytometry. Indeed, pharmacological inhibition of LPA_2 abrogated the effect of LPA in a dose dependent manner resulting in significantly higher percentage of $\gamma H2AX$ positive cells as compared to LPA treatment alone (Fig. 2C). Similar results were obtained using immunofluorescence staining followed by confocal microscopy of $\gamma H2AX$-positive nuclei of IEC-6 cells grown on coverslips treated with the LPA_2 antagonist (supplementary figures 1 A and B).

Activation of the LPA_2 GPCR enhances the kinetics of DNA damage repair

LPA_2-MEF cells are sensitive to radiation-induced apoptosis and can be rescued by postirradiation administration of LPA_2 agonists as shown previously [19, 22]. To dissect the interplay between LPA_2 receptor and DNA damage repair, we used LPA_2- and Vector MEF cells serum starved for 2 hours and treated with 10 μM LPA or vehicle for 15 minutes before exposure to 15 Gy of γ-irradiation at a dose rate of 4.4 Gy/min. Cell lysates were prepared at different time points after irradiation and subjected to western blot analysis to detect $\gamma H2AX$ (figure 3A). Of note that in both cell lines radiation induced comparable levels of H2AX phosphorylation with a peak at 1 hour after irradiation regardless of LPA treatment, indicating that the absence of LPA_2 does not influence the activation of DDR pathway. However, at later time points, at 2 and 4 h, treatment with 10 μM LPA reduced the level and accelerated reduction/resolution of the phosphorylation of H2AX in LPA_2-MEF compared to Vector MEF providing strong evidence for the involvement of LPA_2 in the DNA damage repair pathway.

It is well documented that the prosurvival effects elicited by LPA_2 are mediated in part through the classical G-protein-coupled signals and also the ternary macromolecular signaling complex formed between LPA_2-TRIP6-NHERF2 [25, 32]. First, we examined the involvement of the classical PTX-sensitive G-protein signaling pathway in the resolution kinetics of $\gamma H2AX$ in LPA treated LPA_2-MEF cells. PTX treatment (100 ng/mL) diminished the activation of AKT and ERK, and also delayed the resolution of $\gamma H2AX$ (figure 3B). This result is consistent with a mechanism that a component of the LPA_2-DNA damage signaling pathway involves the PTX sensitive $G_{i/0}$ heterotrimeric G proteins.

Next, to assess the contribution of the LPA_2-TRIP6-NHERF2 ternary macromolecular signaling complex in the DNA damage repair we used MEF reconstituted with wild type LPA_2 or the C311A/C314A/L351A LPA_2 mutant (CACALA-MEF), which is deficient in the assembly of the ternary complex [25]. In LPA_2-MEF versus CACALA MEF LPA-activated AKT and ERK showed different kinetics after IR treatment. In CACALA MEF the intensity of ERK and AKT phosphorylation peaked at the early 15 min time point and slowly decreased thereafter. In contrast in LPA_2-MEF the trend was different showing a slow but sustained activation, which correlated with a faster decrease of $\gamma H2AX$ compared to that found in the MEF expressing the triple mutant LPA_2 (figure 3C). This result is consistent with a previous report that established a role of TRIP6 activation in the amplification and maintenance of ERK1/2 activation in response to LPA stimulation [25].

Finally, to confirm that LPA-induced dephosphorylation of $\gamma H2AX$ depends directly on the activity of the PI3K/AKT and MEK1/ERK pathways we pretreated cells with the PI3K inhibitor LY294002 (10 μM) and the MEK1 inhibitor U0126 (20 μM) for 15 minutes prior

to 15 Gy irradiation. AKT, ERK and H2AX phosphorylation were assessed by western blotting 4 h after irradiation. In the presence of PI3K or MEK1 inhibitors resolution of γH2AX was inhibited (figure 4A).

Sustained ERK1/2 activation is a prerequisite for cell cycle progression and cell proliferation after the DSB repair is completed [33]. We compared ERK activation over an 8 h-long post-irradiation period in LPA$_2$-MEF and Vector MEF. In Vector MEF LPA induced a limited and transient phosphorylation of ERK1/2 with a maximal intensity at 2 h. In contrast, in the LPA2-MEF a robust and sustained ERK activation was present even after 8 h post LPA treatment (figure 4B & insert).

LPA$_2$ knockout mice are deficient in DNA damage repair

We have shown previously that LPA$_2$-specific agonists can mitigate the HE-ARS by rescuing the hematopoietic stem cell compartment from apoptosis [20, 22]. Furthermore, LPA$_2$-KO mice show increased rate of radiation-induced apoptosis, diminished crypt survival in the intestine and increased mortality due to the GI-ARS [13]. Based on these findings we hypothesized that the increased mortality in LPA$_2$-KO mice might be due to the lack of LPA$_2$-mediated DNA damage repair. LPA$_2$ was found to be expressed on Lin-cKit +Sca1+ stem cells and common myeloid progenitors in mice (figure 5A). Furthermore LPA$_2$ shows the highest expression amongst all the LPA1/2/3/4/5 receptors in human CD34$^+$ hematopoietic progenitor cells [22]. To extend our *in vitro* observations concerning the role of LPA$_2$ in DDR described above to a murine radiation injury model we irradiated WT and LPA$_2$-KO mice with 6 Gy at a dose rate of 0.80 Gy/min and measured γH2AX expression in the bone marrow 15 minutes, 4 h and 24 h post-irradiation using flow-cytometry (figure 5B). LPA$_2$-KO mice showed significantly higher residual γH2AX^{high} levels compared to bone marrow cells from WT mice supporting the importance of LPA$_2$ in the repair process. Immunohistological staining of γH2AX in jejunum sections from these mice showed similar difference between WT and LPA$_2$-KO mice 4 h post-irradiation (figures 5C-F).

Radiation increases ATX activity and LPA level in plasma

Augmentation of DNA repair requires ligand activation of LPA$_2$ *in vitro*. The circulating steady-state concentration of LPA in plasma is in the low nanomolar range. To determine if γ-irradiation affects LPA production via ATX, we measured the ATX activity and LPC/LPA content of plasma, WAT, and liver tissues in sham-irradiated and mice exposed to 6 Gy. Four h after irradiation, individual LPA plasma concentrations of the 18:0, 18:1, 18:2, 20:4 and 22:6 molecular species each showed modest elevation in the irradiated plasma samples although they were not significant (figure 6A). However, the 16:0 species and the cumulative LPA concentration of these species was elevated significantly ($p < 0.05$) in the pooled irradiated samples. We could not detect significant difference in plasma LPC content for the same molecular species as those we measured of LPA (figure 6B). The WAT has been shown to be a source of plasma LPA and for this reason we also quantified LPA species in this tissue. In the WAT samples, only the 18:2 molecular species of LPA showed a significant increase (figure 6C). Among the molecular species of LPC, 16:0, 18:1, 18:2 and 20:4 showed significant elevation resulting in a significant difference in the total LPC content compared to non-irradiated samples (figure 6D). In the liver all measured LPA

species showed decreases but only LPA 16:0 was significant together with the total LPA content (Figure 6E). Among the LPC species measured all but the 16:0 species showed significant decreases (figure 6F).

Because ATX is thought to be responsible for the regulation of plasma LPA level and we have found a slight but significant increase in the steady-state level of plasma LPA in the irradiated mice we also measured ATX activity in plasma, WAT, and liver (figure 7). The activity of ATX in plasma but not in WAT or in liver tissues showed a significant elevation in irradiated mice that might explain the slight increase in plasma LPA concentration. Radiation injury has been documented to cause elevation in circulating TNFα levels [34, 35]. TNFα is known to be a robust inducer of ATX transcription [36]. Based on these reports we hypothesized that TNFα generated in irradiated tissues could be involved at least in part in the transcriptional upregulation of ATX and the subsequent increase in ATX activity. To test this hypothesis, we treated IEC-6 cells with 10 ng/ml TNFα and quantified ATX transcripts using QPCR (figure 7B). TNFα treatment after 15 min was accompanied by a significant increase in ATX transcripts and continued to increase up to 24 h the last time point tested. ATX activity in the 24 h conditioned medium showed a significant increase in the TNFα treated sample compared to the untreated control medium (Fig. 7C). These results together suggest that ATX is also upregulated by γ-irradiation and this might at least in part involve TNFα-induced transcriptional activity mediated by NF-κB.

Discussion

Stimulation of the LPA_2 receptor by a variety of selective and specific agonists has been shown to mitigate HE- and GI-ARS [13, 19, 20, 22]. We have recently reported that the LPA_2 specific agonist DBIBB decreased radiation-induced apoptosis in the small intestine, increased crypt regeneration and promoted recovery of the hematopoietic compartment [22]. In the present study we examined whether exposure to γ-irradiation affects the expression and function of the ATX-LPA_2 axis in cultured cells and in mice (figure 8). Specifically, we examined the transcriptional regulation of *lpa2* in IEC-6 crypt-derived cells and in crypts isolated from the small intestine of mice. Our results provide extensive evidence for a novel function of LPA_2 in radiation-induced DNA damage repair by showing that γ-irradiation upregulates its expression and activity. Furthermore, we found that γ-irradiation increases plasma ATX activity and LPA level that is in part due to the previously established radiation-induced upregulation of TNFα. These findings identify ATX and LPA_2 as radiation-regulated genes that appear to play a physiological role in DDR (Fig.8).

We found that the abundance of LPA_2 transcripts shows a radiation dose-response relationship and increases with time during the first 24 h. This tight relationship is unexpected and suggests that LPA_2 transcripts may represent an endogenous biodosimeter/ biomarker. Our data suggest that *lpa2* is a radiation responsive gene regulated by the activated ATM kinase via NF-κB in response to radiation-induced genotoxic stress (Fig. 1A, C, & D). Activation of NF-κB has been firmly linked to radiation exposure. The induction of NF-κB activation upon DNA damage depends on NEMO SUMOylation, and ATM activation by DSB [29] and can confer cell survival or apoptosis depending on the activated target genes. Exposure of mice to total body irradiation induces dose dependent NF-κB

activation in a tissue-specific manner [37-39]. In mice exposed to lethal 8.5 Gy dose robust NF-κB activation was detected in brain, liver, and intestine, and moderate activation in heart, lung, spleen, kidney, and testis [39]. Wang et al. have demonstrated that activation of NF-κB protected intestinal epithelial cells of the small intestinal crypts from ionizing radiation induced damage [38]. We showed in two in vitro model systems of murine intestine that lpa2 is upregulated upon radiation and this response is NF-κB dependent. Radiation (4 Gy) induced significant increase in *lpa2* mRNA level in irradiated in vitro cultured intestinal crypts and elicits a time- and dose-dependent transcriptional response in IEC-6 cells, an epithelial cell line of intestinal crypt origin. Site directed mutagenesis of NF-κB binding site in the human *lpa2* promoter abrogated the effect of radiation. Furthermore, we provide evidence that radiation exposure of IEC-6 cells not only increased the abundance of LPA$_2$ transcripts but also increased the responsiveness of the cells to an LPA$_2$-specific agonist indicated by the significantly higher Ca^{2+} responses and the left shift in the dose-response curve. In fact the induction of LPA$_2$ in response to radiation may represent a positive feedback between LPA$_2$ and NF-κB activation.

We used pharmacological inhibition of ATM, the master regulator of DDR, to link LPA$_2$ to DNA damage response. In IEC-6 cells pre-treated with the ATM/ATR kinase inhibitor CGK 733 radiation failed to induce upregulation of *lpa2*. The antiapoptotic effect of LPA$_2$ is well documented [12-14, 18-20], and we have shown previously that the LPA$_2$ specific agonist DBIBB increased the clonogenic capacity of irradiated IEC-6 crypt epithelium-like cells via inhibition of caspase 3/7 activation [22]. The same LPA$_2$ agonist also facilitated the resolution of γH2AX in LPA$_2$ MEF [22]. We show evidence that LPA treatment induces a faster repair kinetics compared to the untreated cells and this effect was blocked completely by a specific LPA$_2$ antagonist excluding the contribution of the other LPA receptors expressed on IEC-6 cells. The antiapoptotic function of LPA$_2$ depends both on the classical, pertussis toxin-sensitive G$_{1/0}$ mediated pathway and on the ligand–induced assembly of a ternary signaling complex that includes LPA$_2$-TRIP6-NHERF2 [19, 25]. Using the LPA$_{1/2}$ double KO-derived MEF stably transduced with either the WT LPA$_2$ or the C-terminus mutated CACALA-LPA$_2$, which is unable to recruit the ternary complex, we demonstrated that the LPA$_2$ -induced DDR requires both of these pathways. The disruption of either pathway results in delayed DNA damage repair indicated by the protracted presence of high γH2AX levels, probably due to accompanying decrease in AKT and ERK activation. The implication of ERK and AKT prosurvival kinase pathways in the LPA$_2$-induced repair is supported by results from the pharmacological inhibition of PI3K with LY294002 and MEK1 with U016, leading to accumulation of γH2AX following treatment with either blocker. Moreover, we showed that LPA treatment induces robust and sustained ERK activity in LPA$_2$-MEF but not in Vector MEF. These results taken together indicate that LPA$_2$ is necessary and sufficient to augment the DDR response.

Although we provide extensive proofs supporting the role of LPA$_2$ in the radiation induced DDR, further studies are needed to elucidate the detailed mechanism linking LPA$_2$ signaling to DSB repair. We hypothesize that DNA-PK could be the convergence point downstream signals from ERK. A recent study demonstrated that in mouse hematopoietic stem and progenitor cells exposed to irradiation and trombopoietin treatment activated ERK and NF-

κB pathways, which in turn induced the upregulation of their common target, the early stress response gene Iex-1, leading to enhancement of DNA-PK activity and nonhomologous end joining (NHEJ) [40]. Kriegs et el [41] reported the role of MAPK signaling in EGFR-mediated DSB repair based on evidence that inhibition of ERK blocked the NHEJ. Although, LPA GPCR have been shown to transactivate EGFR signaling [41, 42], our findings showed that EGFR is not required for the antiapoptotic effect of LPA. Thus, more experiments will be necessary to piece together whether LPA similarly to thrombopoietin induces transcriptional upregulation of *iex-1* and formation of a macromolecular complex between ERK1/2, IEX-1 and DNA-PK.

We also demonstrated that LPA_2 mediates DDR in vivo and the lack of LPA_2 receptor does not influence the activation of DNA damage response pathway in the HE and GI system. Purified hematopoietic stem cells abundantly express LPA_2 transcripts. We measured γH2AX in the bone marrow of LPA_2-KO and WT mice exposed to 6 Gy TBI 15 min, 4 h and 24 h post-irradiation. At the early time points the level of γH2AX was almost identical in bone marrow cells of WT and LPA_2-KO mice pointing to similar activation of the DDR pathway. However, significant difference occurred at 24 h post-irradiation, with a significantly higher residual damage remaining in the bone marrow of the LPA_2-KO mice compared to WT animals. γH2AX staining of jejunum sections from WT and LPA_2-KO C57BL/6 mice 4 h after irradiation showed more residual γH2AX compared to WT mice. This result indicates that in the absence of exogenously added LPA the DDR proceeds more rapidly or achieves a more complete resolution of DSB in WT mice expressing LPA_2 GPCR in their small intestine. LPA is present in and also generated from food [43] and in blood plasma. The exact source of LPA responsible for activation of LPA_2 in enterocytes and intestinal stem cells is unknown at the present time.

In biological fluids, LPA is primarily generated by ATX [44]. In this context we examined LPA and LPC levels in blood plasma, WAT the major source of circulating LPA [45], and the liver that is the site of LPA clearance from blood. The total concentration of circulating plasma LPA showed a significant elevation in irradiated mice compared to sham irradiated controls. In testicular WAT tissue we found that only the LPA 18:2 species showed significant elevation after irradiation. The total LPA content of the liver tissue showed a significant decrease after irradiation. Taking these data together, the possibility arises that irradiation is responsible for the upregulation of ATX activity which in turn elevates plasma LPA concentration. ATX reaction rates in these tissues showed significant radiation-induced elevation only in the plasma (Fig. 8). To date there is no evidence for posttranscriptional physiological regulation of plasma ATX activity. For this reason we hypothesized that the increase in ATX activity of plasma could be due to transcriptional upregulation of the ATX gene. ATX transcription has been shown to be regulated by NF-κB and NFAT [36, 46]. Radiation exposure of animals is known to cause a rapid elevation in TNF-α and IL-6 levels [34, 35]. We hypothesized that radiation-induced TNF-α could be responsible at least in part for the upregulation of ATX. In this context, we also note that ATX is anchored to the cell surface via integrin [47] and heparin binding [48]. Thus, de novo synthesized ATX maintained at the cell surface could generate LPA in a localized manner that in turn activates LPA GPCR in a juxtacrine and/or paracrine manner. Such localized LPA production would

not lead to high elevation in the steady-state concentration of circulating LPA. Because we found an accelerated resolution of γH2AX staining in jejunum sections of irradiated mice we used the IEC-6 cell line to test whether TNF-α upregulates ATX in these cells. TNF-α indeed increased the abundance of ATX transcripts in IEC-6 cells providing circumstantial evidence that such mechanism could take place in vivo too. Further experiments will be required to assess the role of the pro-inflammatory milieu induced by radiation on the transcriptional regulation of LPA_2 and ATX expression.

In a larger context the present findings concerning the radiation-induced upregulation of the ATX-LPA_2 signaling axis, it will be of great interest to investigate how radiation therapy affects ATX activity and LPA production, given that to both ATX and LPA were attributed with playing a major role in metastasis, chemo- and radiation-resistance of several cancers [15, 49-51].

Conclusion

Based on the presented data we propose that the ATX-LPA-LPA_2 axis is a novel, radiation-induced stress response pathway, contributing to DNA damage repair and cell survival following radiation induced genotoxic insult.

Supplementary Material

Refer to Web version on PubMed Central for supplementary material.

Acknowledgement

Abbreviations

DSB	DNA double strand breaks
DDR	DNA damage repair
ATX	lysophospholipase D autotaxin
LPA	lysophosphatidic acid
LPC	lysophosphatidylcholine
ATM	ataxia teleangiectasia mutated kinase
PTX	pertussis toxin
NHEJ	DNA nonhomologous end joining

References

[1]. Bhatti S, Kozlov S, Farooqi AA, Naqi A, Lavin M, Khanna KK. ATM protein kinase: the linchpin of cellular defenses to stress. Cell Mol Life Sci. 2011; 68:2977–3006. [PubMed: 21533982]

[2]. Smith J, Tho LM, Xu N, Gillespie DA. The ATM-Chk2 and ATR-Chk1 pathways in DNA damage signaling and cancer. Adv Cancer Res. 2010; 108:73–112. [PubMed: 21034966]

[3]. Tentner AR, Lee MJ, Ostheimer GJ, Samson LD, Lauffenburger DA, Yaffe MB. Combined experimental and computational analysis of DNA damage signaling reveals context-dependent roles for Erk in apoptosis and G1/S arrest after genotoxic stress. Mol Syst Biol. 2012; 8:568. [PubMed: 22294094]

[4]. Lin ME, Herr DR, Chun J. Lysophosphatidic acid (LPA) receptors: signaling properties and disease relevance. Prostaglandins Other Lipid Mediat. 2010; 91:130–138. [PubMed: 20331961]

[5]. Yanagida K, Kurikawa Y, Shimizu T, Ishii S. Current progress in non-Edg family LPA receptor research. Biochim Biophys Acta. 2013; 1831:33–41. [PubMed: 22902318]

[6]. Houben AJ, Moolenaar WH. Autotaxin and LPA receptor signaling in cancer. Cancer Metastasis Rev. 2011; 30:557–565. [PubMed: 22002750]

[7]. Tager AM. Autotaxin emerges as a therapeutic target for idiopathic pulmonary fibrosis: limiting fibrosis by limiting lysophosphatidic acid synthesis. Am J Respir Cell Mol Biol. 2012; 47:563–565. [PubMed: 23125419]

[8]. Moolenaar WH, Houben AJ, Lee SJ, van Meeteren LA. Autotaxin in embryonic development. Biochim Biophys Acta. 2013; 1831:13–19. [PubMed: 23022664]

[9]. Evseenko D, Latour B, Richardson W, Corselli M, Sahaghian A, Cardinal S, Zhu Y, Chan R, Dunn B, Crooks GM. Lysophosphatidic acid mediates myeloid differentiation within the human bone marrow microenvironment. PLoS One. 2013; 8:e63718. [PubMed: 23696850]

[10]. Ortlepp C, Steudel C, Heiderich C, Koch S, Jacobi A, Ryser M, Brenner S, Bornhauser M, Brors B, Hofmann WK, Ehninger G, Thiede C. Autotaxin is expressed in FLT3-ITD positive acute myeloid leukemia and hematopoietic stem cells and promotes cell migration and proliferation. Exp Hematol. 2013; 41:444–461. e444. [PubMed: 23377000]

[11]. Costa M, Sourris K, Lim SM, Yu QC, Hirst CE, Parkington HC, Jokubaitis VJ, Dear AE, Liu HB, Micallef SJ, Koutsis K, Elefanty AG, Stanley EG. Derivation of endothelial cells from human embryonic stem cells in fully defined medium enables identification of lysophosphatidic acid and platelet activating factor as regulators of eNOS localization. Stem Cell Res. 2013; 10:103–117. [PubMed: 23164599]

[12]. Deng W, Balazs L, Wang DA, Van Middlesworth L, Tigyi G, Johnson LR. Lysophosphatidic acid protects and rescues intestinal epithelial cells from radiation- and chemotherapy-induced apoptosis. Gastroenterology. 2002; 123:206–216. [PubMed: 12105849]

[13]. Deng W, Shuyu E, Tsukahara R, Valentine WJ, Durgam G, Gududuru V, Balazs L, Manickam V, Arsura M, VanMiddlesworth L, Johnson LR, Parrill AL, Miller DD, Tigyi G. The lysophosphatidic acid type 2 receptor is required for protection against radiation-induced intestinal injury. Gastroenterology. 2007; 132:1834–1851. [PubMed: 17484878]

[14]. Deng W, Wang DA, Gosmanova E, Johnson LR, Tigyi G. LPA protects intestinal epithelial cells from apoptosis by inhibiting the mitochondrial pathway. Am J Physiol Gastrointest Liver Physiol. 2003; 284:G821–829. [PubMed: 12684213]

[15]. Brindley DN, Lin FT, Tigyi GJ. Role of the autotaxin-lysophosphatidate axis in cancer resistance to chemotherapy and radiotherapy. Biochim Biophys Acta. 2013; 1831:74–85. [PubMed: 22954454]

[16]. Yang SY, Lee J, Park CG, Kim S, Hong S, Chung HC, Min SK, Han JW, Lee HW, Lee HY. Expression of autotaxin (NPP-2) is closely linked to invasiveness of breast cancer cells. Clin Exp Metastasis. 2002; 19:603–608. [PubMed: 12498389]

[17]. Yang Y, Mou L, Liu N, Tsao MS. Autotaxin expression in non-small-cell lung cancer. Am J Respir Cell Mol Biol. 1999; 21:216–222. [PubMed: 10423404]

[18]. Kiss GN, Fells JI, Gupte R, Lee SC, Liu J, Nusser N, Lim KG, Ray RM, Lin FT, Parrill AL, Sumegi B, Miller DD, Tigyi G. Virtual screening for LPA2-specific agonists identifies a nonlipid compound with antiapoptotic actions. Mol Pharmacol. 2012; 82:1162–1173. [PubMed: 22968304]

[19]. Kiss GN, Lee SC, Fells JI, Liu J, Valentine WJ, Fujiwara Y, Thompson KE, Yates CR, Sumegi B, Tigyi G. Mitigation of radiation injury by selective stimulation of the LPA(2) receptor. Biochim Biophys Acta. 2013; 1831:117–125. [PubMed: 23127512]

[20]. Deng W, Kimura Y, Gududuru V, Wu W, Balogh A, Szabo E, Thompson KE, Yates CR, Balazs L, Johnson LR, Miller DD, Strobos J, McCool WS, Tigyi GJ. Mitigation of the Hematopoietic and Gastrointestinal Acute Radiation Syndrome by Octadecenyl Thiophosphate, a Small Molecule Mimic of Lysophosphatidic Acid. Radiat Res. 2015 DOI 10.1667/RR13830.1.

[21]. Patil R, Fells JI, Szabo E, Lim KG, Norman DD, Balogh A, Patil S, Strobos J, Miller DD, Tigyi GJ. Design and synthesis of sulfamoyl benzoic acid analogues with subnanomolar agonist activity specific to the LPA2 receptor. J Med Chem. 2014; 57:7136–7140. [PubMed: 25100502]

[22]. Patil R, Szabo E, Fells JI, Balogh A, Lim KG, Fujiwara Y, Norman DD, Lee SC, Balazs L, Thomas F, Patil S, Emmons-Thompson K, Boler A, Strobos J, McCool SW, Yates CR, Stabenow J, Byrne GI, Miller DD, Tigyi GJ. Combined mitigation of the gastrointestinal and hematopoietic acute radiation syndromes by an LPA2 receptor-specific nonlipid agonist. Chem Biol. 2015; 22:206–216. [PubMed: 25619933]

[23]. Deng W, Poppleton H, Yasuda S, Makarova N, Shinozuka Y, Wang DA, Johnson LR, Patel TB, Tigyi G. Optimal lysophosphatidic acid-induced DNA synthesis and cell migration but not survival require intact autophosphorylation sites of the epidermal growth factor receptor. J Biol Chem. 2004; 279:47871–47880. [PubMed: 15364923]

[24]. Lin FT, Lai YJ, Makarova N, Tigyi G, Lin WC. The lysophosphatidic acid 2 receptor mediates down-regulation of Siva-1 to promote cell survival. J Biol Chem. 2007; 282:37759–37769. [PubMed: 17965021]

[25]. E S, Lai YJ, Tsukahara R, Chen CS, Fujiwara Y, Yue J, Yu JH, Guo H, Kihara A, Tigyi G, Lin FT. Lysophosphatidic acid 2 receptor-mediated supramolecular complex formation regulates its antiapoptotic effect. J Biol Chem. 2009; 284:14558–14571. [PubMed: 19293149]

[26]. Beck HP, Kohn T, Rubenstein S, Hedberg C, Schwandner R, Hasslinger K, Dai K, Li C, Liang L, Wesche H, Frank B, An S, Wickramasinghe D, Jaen J, Medina J, Hungate R, Shen W. Discovery of potent LPA2 (EDG4) antagonists as potential anticancer agents. Bioorg Med Chem Lett. 2008; 18:1037–1041. [PubMed: 18178086]

[27]. Okudaira M, Inoue A, Shuto A, Nakanaga K, Kano K, Makide K, Saigusa D, Tomioka Y, Aoki J. Separation and quantification of 2-acyl-1-lysophospholipids and 1-acyl-2-lysophospholipids in biological samples by LC-MS/MS. J Lipid Res. 2014; 55:2178–2192. [PubMed: 25114169]

[28]. Rusovici R, Ghaleb A, Shim H, Yang VW, Yun CC. Lysophosphatidic acid prevents apoptosis of Caco-2 colon cancer cells via activation of mitogen-activated protein kinase and phosphorylation of Bad. Biochim Biophys Acta. 2007; 1770:1194–1203. [PubMed: 17544220]

[29]. McCool KW, Miyamoto S. DNA damage-dependent NF-kappaB activation: NEMO turns nuclear signaling inside out. Immunol Rev. 2012; 246:311–326. [PubMed: 22435563]

[30]. Tanaka T, Halicka D, Traganos F, Darzynkiewicz Z. Cytometric analysis of DNA damage: phosphorylation of histone H2AX as a marker of DNA double-strand breaks (DSBs). Methods Mol Biol. 2009; 523:161–168. [PubMed: 19381940]

[31]. Sharma A, Singh K, Almasan A. Histone H2AX phosphorylation: a marker for DNA damage. Methods Mol Biol. 2012; 920:613–626. [PubMed: 22941631]

[32]. Radeff-Huang J, Seasholtz TM, Matteo RG, Brown JH. G protein mediated signaling pathways in lysophospholipid induced cell proliferation and survival. J Cell Biochem. 2004; 92:949–966. [PubMed: 15258918]

[33]. Yamamoto T, Ebisuya M, Ashida F, Okamoto K, Yonehara S, Nishida E. Continuous ERK activation downregulates antiproliferative genes throughout G1 phase to allow cell-cycle progression. Curr Biol. 2006; 16:1171–1182. [PubMed: 16782007]

[34]. Girinsky TA, Pallardy M, Comoy E, Benassi T, Roger R, Ganem G, Cosset JM, Socie G, Magdelenat H. Peripheral blood corticotropin-releasing factor, adrenocorticotropic hormone and cytokine (interleukin beta, interleukin 6, tumor necrosis factor alpha) levels after high- and low-dose total-body irradiation in humans. Radiat Res. 1994; 139:360–363. [PubMed: 8073120]

[35]. Schaue D, Kachikwu EL, McBride WH. Cytokines in radiobiological responses: a review. Radiat Res. 2012; 178:505–523. [PubMed: 23106210]

[36]. Wu JM, Xu Y, Skill NJ, Sheng H, Zhao Z, Yu M, Saxena R, Maluccio MA. Autotaxin expression and its connection with the TNF-alpha-NF-kappaB axis in human hepatocellular carcinoma. Mol Cancer. 2010; 9:71. [PubMed: 20356387]

[37]. Zhou D, Brown SA, Yu T, Chen G, Barve S, Kang BC, Thompson JS. A high dose of ionizing radiation induces tissue-specific activation of nuclear factor-kappaB in vivo. Radiat Res. 1999; 151:703–709. [PubMed: 10360790]

[38]. Wang Y, Meng A, Lang H, Brown SA, Konopa JL, Kindy MS, Schmiedt RA, Thompson JS, Zhou D. Activation of nuclear factor kappaB In vivo selectively protects the murine small intestine against ionizing radiation-induced damage. Cancer Res. 2004; 64:6240–6246. [PubMed: 15342410]

[39]. Chang CT, Lin H, Ho TY, Li CC, Lo HY, Wu SL, Huang YF, Liang JA, Hsiang CY. Comprehensive assessment of host responses to ionizing radiation by nuclear factor-kappaB bioluminescence imaging-guided transcriptomic analysis. PLoS One. 2011; 6:e23682. [PubMed: 21887294]

[40]. de Laval B, Pawlikowska P, Barbieri D, Besnard-Guerin C, Cico A, Kumar R, Gaudry M, Baud V, Porteu F. Thrombopoietin promotes NHEJ DNA repair in hematopoietic stem cells through specific activation of Erk and NF-kappaB pathways and their target, IEX-1. Blood. 2014; 123:509–519. [PubMed: 24184684]

[41]. Lowenstein EJ, Daly RJ, Batzer AG, Li W, Margolis B, Lammers R, Ullrich A, Skolnik EY, Bar-Sagi D, Schlessinger J. The SH2 and SH3 domain-containing protein GRB2 links receptor tyrosine kinases to ras signaling. Cell. 1992; 70:431–442. [PubMed: 1322798]

[42]. Prenzel N, Zwick E, Daub H, Leserer M, Abraham R, Wallasch C, Ullrich A. EGF receptor transactivation by G-protein-coupled receptors requires metalloproteinase cleavage of proHB-EGF. Nature. 1999; 402:884–888. [PubMed: 10622253]

[43]. Nakane S, Tokumura A, Waku K, Sugiura T. Hen egg yolk and white contain high amounts of lysophosphatidic acids, growth factor-like lipids: distinct molecular species compositions. Lipids. 2001; 36:413–419. [PubMed: 11383695]

[44]. Umezu-Goto M, Kishi Y, Taira A, Hama K, Dohmae N, Takio K, Yamori T, Mills GB, Inoue K, Aoki J, Arai H. Autotaxin has lysophospholipase D activity leading to tumor cell growth and motility by lysophosphatidic acid production. J Cell Biol. 2002; 158:227–233. [PubMed: 12119361]

[45]. Dusaulcy R, Rancoule C, Gres S, Wanecq E, Colom A, Guigne C, van Meeteren LA, Moolenaar WH, Valet P, Saulnier-Blache JS. Adipose-specific disruption of autotaxin enhances nutritional fattening and reduces plasma lysophosphatidic acid. J Lipid Res. 2011; 52:1247–1255. [PubMed: 21421848]

[46]. Chen M, O'Connor KL. Integrin alpha6beta4 promotes expression of autotaxin/ENPP2 autocrine motility factor in breast carcinoma cells. Oncogene. 2005; 24:5125–5130. [PubMed: 15897878]

[47]. Wu T, Kooi CV, Shah P, Charnigo R, Huang C, Smyth SS, Morris AJ. Integrin-mediated cell surface recruitment of autotaxin promotes persistent directional cell migration. FASEB J. 2014; 28:861–870. [PubMed: 24277575]

[48]. Houben AJ, van Wijk XM, van Meeteren LA, van Zeijl L, van de Westerlo EM, Hausmann J, Fish A, Perrakis A, van Kuppevelt TH, Moolenaar WH. The polybasic insertion in autotaxin alpha confers specific binding to heparin and cell surface heparan sulfate proteoglycans. J Biol Chem. 2013; 288:510–519. [PubMed: 23150666]

[49]. Schleicher SM, Thotala DK, Linkous AG, Hu R, Leahy KM, Yazlovitskaya EM, Hallahan DE. Autotaxin and LPA receptors represent potential molecular targets for the radiosensitization of murine glioma through effects on tumor vasculature. PLoS One. 2011; 6:e22182. [PubMed: 21799791]

[50]. Leblanc R, Peyruchaud O. New insights into the autotaxin/LPA axis in cancer development and metastasis. Exp Cell Res. 2015; 333:183–189. [PubMed: 25460336]

[51]. Lee SC, Fujiwara Y, Liu J, Yue J, Shimizu Y, Norman DD, Wang Y, Tsukahara R, Szabo E, Patil R, Banerjee S, Miller DD, Balazs L, Ghosh MC, Waters CM, Oravecz T, Tigyi GJ. Autotaxin and LPA1 and LPA5 receptors exert disparate functions in tumor cells versus the host tissue microenvironment in melanoma invasion and metastasis. Mol Cancer Res. 2015; 13:174–185. [PubMed: 25158955]

Highlights

- γ-irradiation upregulates ATX and LPA$_2$ expression.

- Plasma ATX activity and LPA are elevated in irradiated mice.

- Upregulation of ATX and LPA$_2$ are mediated by NF-κB.

- Resolution γH2AX is accelerated by LPA$_2$ activation in vivo.

- LPA$_2$-mediated augmentation of γH2AX resolution involves AKT, ERK1/2, and assembly of a C-terminal macromolecular signaling complex.

- ATX and LPA$_2$ upregulation play a role in endogenous DNA damage repair.
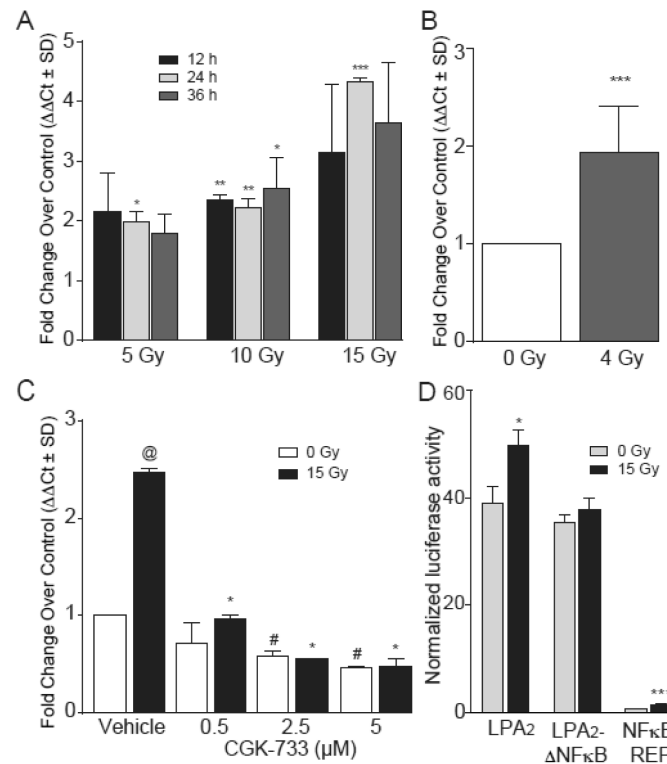
Figure 1. *lpa2* is a radiation responsive gene that is time- and dose-dependently upregulated in response to γ-irradiation via an ATM-mediated NF-κB activation

Panel A. Quantitative RT-PCR analysis of *lpa2* expression in cultured IEC-6 irraditated with 5, 10 and 15 Gy at 12, 24 and 36 h. *P < 0.05 between irradiated and non-irradiated samples of each time point. **Panel B.** *lpa2* gene expression measured by qRT-PCR in cultured intestinal crypts 24 h after 4 Gy irradiation. **Panel C.** Quantitative RT-PCR of *lpa2* expression 24 h post-irradiation in IEC-6 cells treated with increasing concentration of the ATM/ATR kinase inhibitor CGK-733 30 min prior to 15 Gy irradiation. *P < 0.05 between irradiated and irradiated samples treated with CGK-733, @ P < 0.05 between 0 Gy and 15 Gy, # P < 0.05 between 0 Gy samples treated or non-treated with CGK-733. **Panel D.** Mutation of a putative NF-κB –binding site present in the human *lpa2* promoter results in abrogation of radiation induced upregulation of transcriptional activity measured with the luciferase promoter assay. Data represents the mean of two experiments ± SD performed in triplicate. *P < 0.05 between irradiated and control samples.
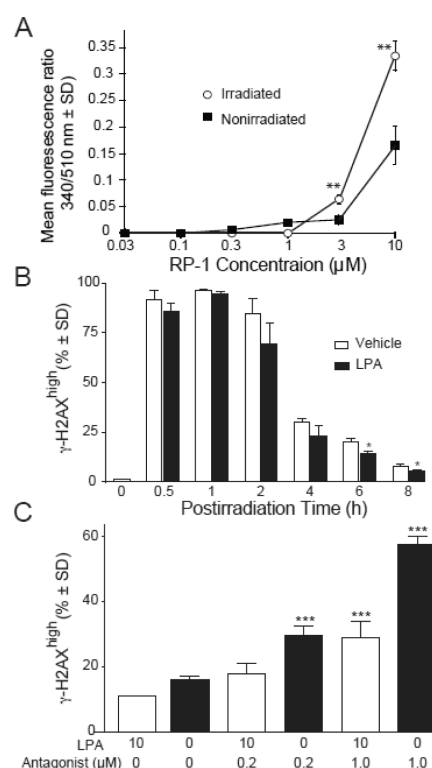
Figure 2. LPA$_2$ is functionally upregulated and it maintains its functionality after irradiation as measured by Ca^{2+} assay

Panel A. IEC-6 cells irradiated with 15 Gy were treated with an LPA$_2$ specific agonist 24 h later to elicit a Ca^{2+} response. Data represents the mean of two experiments ± SD performed in triplicate. Statistical analysis of the data between the groups was performed by a Student's t-test. *P < 0.05. **Panel B.** The LPA$_2$ receptor accelerates the repair kinetics of DNA damage. Kinetics of γH2AX formation and resolution in irradiated IEC-6 cells treated with 10μM LPA for 15 minutes prior to irradiation. γH2AX was measured at the indicated time points by flow cytometry. **Panel C.** Pharmacological inhibition of LPA$_2$ dose-dependently abrogates the effect of LPA. Cells were treated with 0.2μM and 1μM LPA$_2$ antagonist Amgen compound 35 (ANT) 30 min prior to the addition of 10 μM LPA or vehicle 15 min before irradiation with 15 Gy. γH2AX was measured 6 h after irradiation with flow cytometry. Data shown are representative of three experiments. Statistical analysis of the data between the groups was performed by a Student's t-test. *P < 0.05.
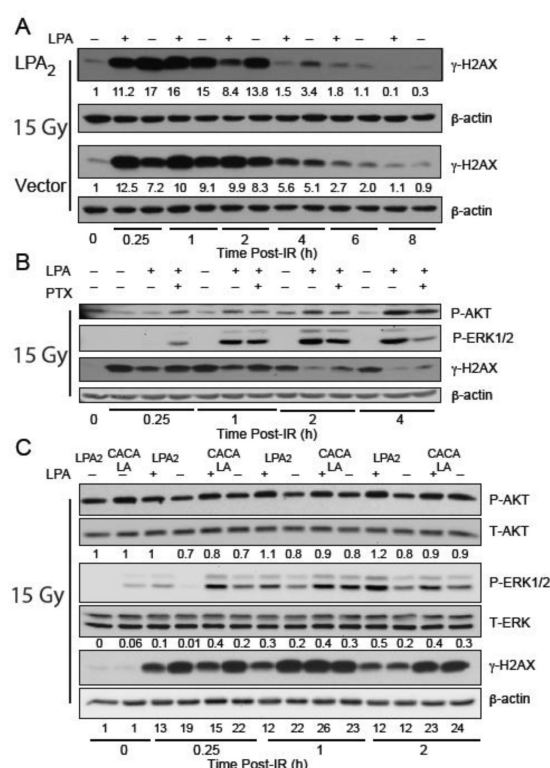
Figure 3. LPA$_2$ facilitates the radiation induced DNA damage repair in part via the classical G-protein-coupled signals and also the ternary macromolecular complex between LPA$_2$-TRIP6-NHERF2 indicated by γH2AX levels detected by Western blotting

Panel A. Time-course of γH2AX resolution in LPA$_2$-MEF (LPA$_2$) and Vector MEF preincubated with 10 μM LPA and irradiated with 15 Gy confirms the role of LPA$_2$ in DNA damage repair with a 10 × higher residual γH2AX expression level in Vector MEF 8 h post-IR treatment. **Panel B**. Inhibition of G$_{i/0}$ heterotrimeric G proteins with PTX in LPA$_2$-MEFs prior to irradiation treatment (15 Gy) results in reduced AKT and ERK1&2 activation and accumulation of γH2AX. **Panel C.** Disruption of the ternary macromolecular signaling complex formed between LPA2-TRIP6-NHERF2 in the CACALA-MEFs pretreated for 15 minutes with either 10 μM LPA or vehicle and irradiated with 15 Gy results in reduced AKT and ERK1&2 activation and a subsequent γH2AX accumulation. Arbitrary units represent light intensity values measured by Image J software and normalized to β-actin and calculated as fold over non-irradiated control.
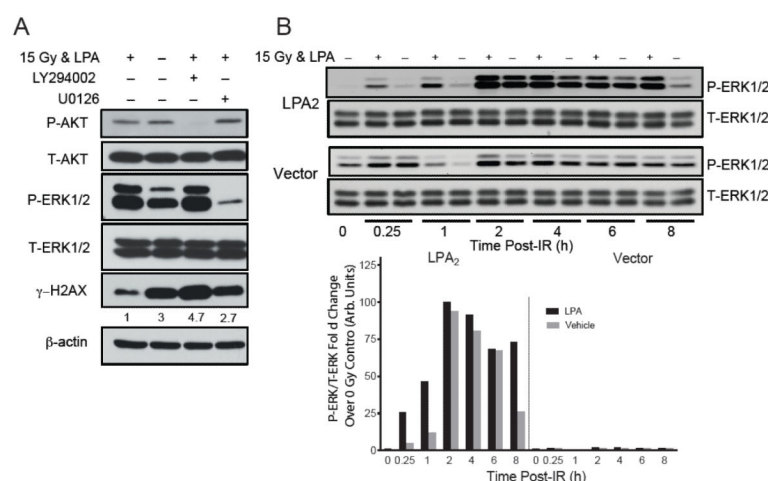
**Figure 4. Pharmacological inhibition of AKT or ERK 1&2 activation confirms their role in LPA$_2$ mediated DDR**

Panel A. LPA$_2$-MEFs were treated with either 10 μM of the PI3K inhibitor LY294002 or 20 μM of the MEK1 inhibitor U0126 for 30 min before addition of 10 μM LPA for 15 min prior to irradiation (15 Gy). In the presence of PI3K or MEK1 inhibitors concomitant with AKT and ERK1&2 inhibition the repair process was also delayed marked by increased accumulation of γH2AX 4 hours after irradiation compared with the LPA only treated samples. **Panel B.** LPA$_2$ activation confers sustained ERK1&2 phosphorylation, a prerequisite for cell cycle progression. Arbitrary units represent light intensity values measured by Image J software and normalized to β-actin and calculated as fold over non-irradiated control. Blots are representative of two other experiments.
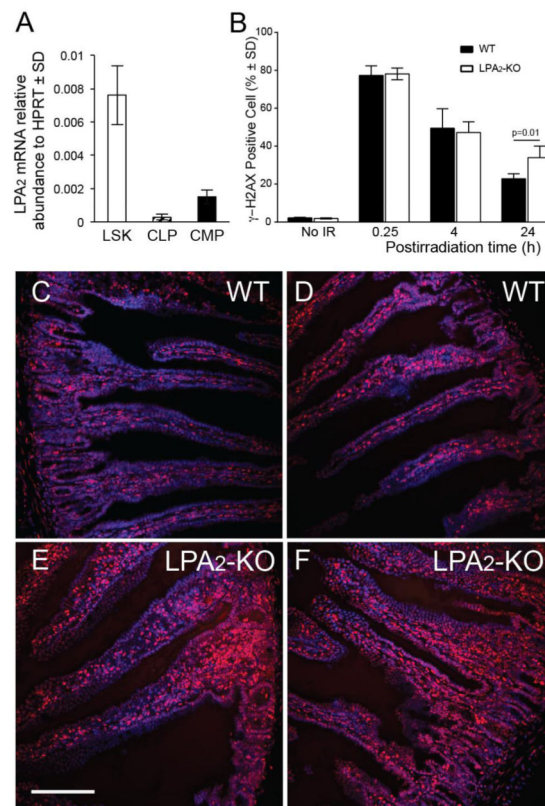
Figure 5. The role of LPA$_2$ in DDR of HE stem/progenitor cells and in the jejunum
Panel A. *lpa2* expression detected by qRT-PCR analysis on stem (LSK) and lymphoid
(CLP) and myeloid progenitor cell populations (CMP) from murine bone marrow. **Panel B.**
LPA$_2$-KO mice are deficient in the DDR process. Bone marrow isolated from mice exposed
to 6 Gy TBI was subjected to flow cytometric analysis 15 minutes, 4 and 24 h
postirradiation to determine γH2AX positive cells. LPA$_2$-KO mice show elevated residual
γH2AX compared to WT mice 24 h after 6 Gy total body irradiation. Representative of two
experiments, n= 5 mice. *Denotes p value < 0.05 calculated by Student's t-test. **Panel C.**
γH2AX immunostaining in the jejuni of WT and LPA$_2$-KO mice 4 h after 6 Gy total body
irradiation shows elevated γH2AX expression in LPA$_2$-KO mice compared to WT (γH2AX
foci are stained red, nuclei are blue). Calibration bar = 250 μm.
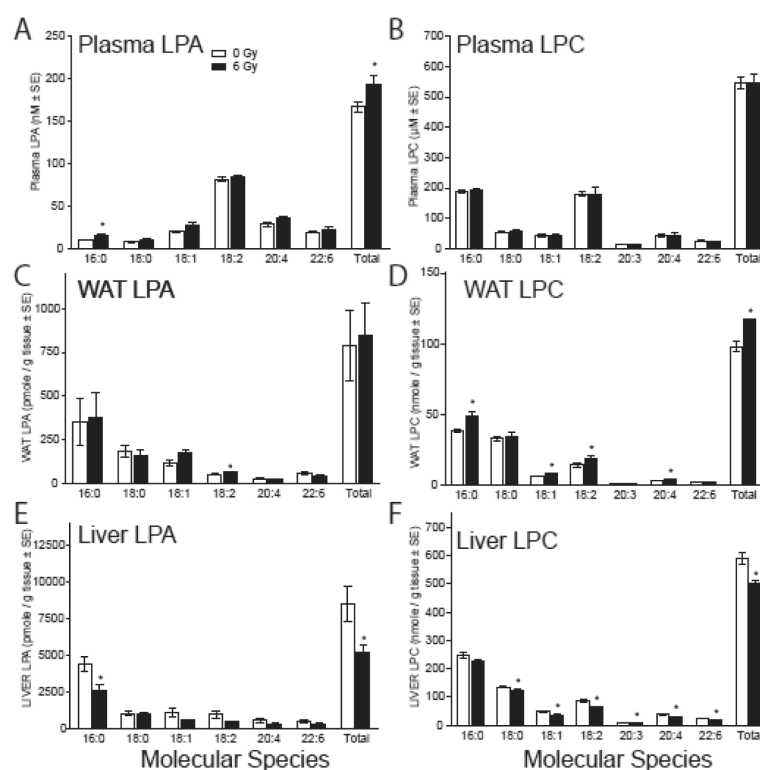
Figure 6. Radiation induced changes in LPA and LPC content of plasma (A & B), WAT (C & D), and liver tissue (E & F)

LPC and LPA were extracted from plasma, WAT and livers of mice exposed to 6 Gy total body irradiation 4 h post-irradiation. LPC and LPA content were determined by LC-MS/MS. Statistical analysis of the data between the groups was performed by ANOVA with Bonferoni's post test. *P < 0.05, n = 5 mice.
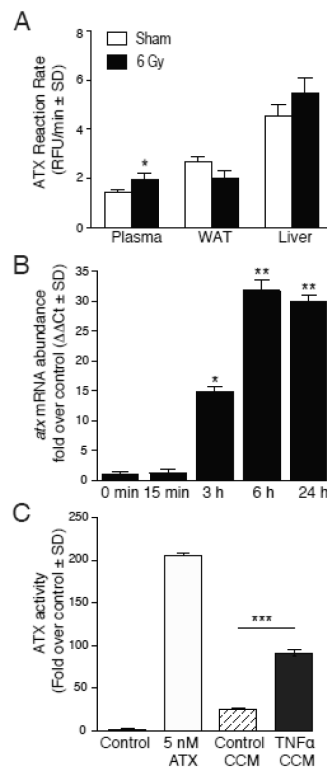
Figure 7. ATX expression and enzyme activity is upregulated in response to TNF-α
Panel A. ATX reaction rate in irradiated mouse plasma, WAT, and liver samples of mice irradiated with 6 Gy at 4 h post-exposure. Average reaction rates were compared between vehicle and irradiation treatment using one-factor ANOVA with Bonferroni's post-test to determine if rates differed significantly versus non-irradiated control. * $P < 0.05$. For plasma samples, n = 10 mice with * denoting $p < 0.05$ statistical significance. For tissue samples, n = 5 mice. **Panel B.** Quantitative RT-PCR analysis of *atx* gene expression in cultured IEC-6 stimulated with 10ng/ml TNFα for the indicated time points. Average mRNA abundance were compared via ANOVA with Bonferroni's post-test to identify significant differences versus T_0 control. * $P < 0.05$; ** $P < 0.001$. **Panel C.** ATX activity was measured in concentrated conditioned medium (CCM) of IEC-6 cells stimulated with or without 10ng/ml TNFα for 24 hours. Negative control contains fluorescent substrate FS-3 alone, whereas 5 nM recombinant purified ATX was used as a positive control for the assay. Control CCM (CTL CCM) was generated from IEC-6 cells not exposed to TNFα stimulation. The change in fluorescent intensity was monitored over 4 hours at 37°C using the FlexStation II. The differences in ATX activity between 4-h end- and 0-h start-point were calculated and normalized to negative control and ANOVA was paired with Bonferroni's post-test to determine if reaction rates significantly differed. *** $P < 0.0001$
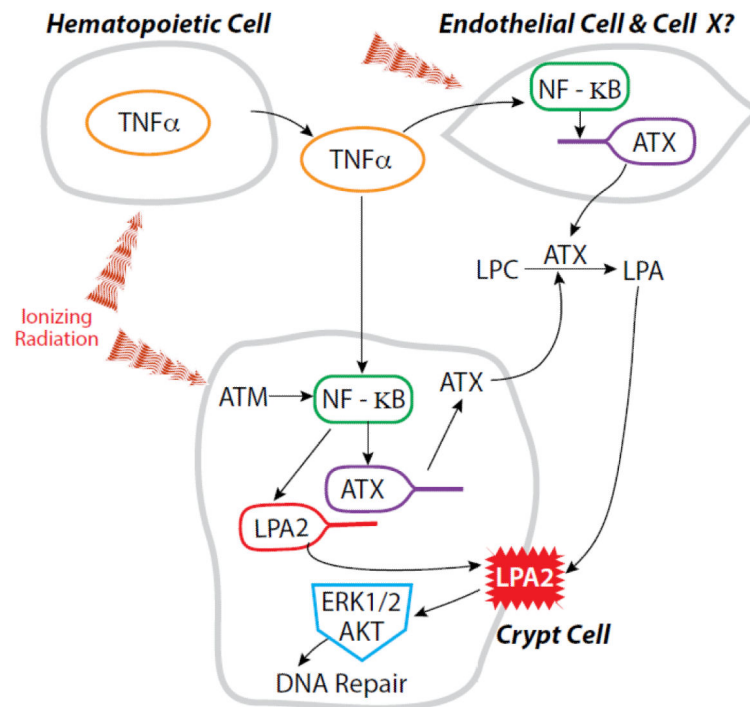
Figure 8. Working hypothesis for the regulation of the ATX-LPA$_2$ axis in response to γ-radiation
Radiation is known to induce the release of proinflammatory cytokines such as TNFα by hematopoietic cells into the blood which could upregulate ATX production through NF-κB in the endothelial lining of blood vessels and other yet to be identified target cells. This results in increased ATX enzyme activity and subsequent LPA content of plasma. In intestinal stem cell like cells, modeled by the IEC-6 cell line, the LPA$_2$ receptor is upregulated in response to radiation induced DNA damage via an ATM- NF-κB dependent pathway. At the same time, ATX production is upregulated by the radiation-induced release of TNFα into the circulation. The elevated LPA content and receptor upregulation drives the enhanced DNA damage repair.